EPSC Abstracts
Vol. 16, EPSC2022-646, 2022, updated on 30 Nov 2022
https://doi.org/10.5194/epsc2022-646
Europlanet Science Congress 2022

Homogeneous versus heterogeneous lunar mantle: Constraints from secondary crust production

Irene Bernt, **Ana-Catalina Plesa**, Sabrina Schwinger, Max Collinet, and Doris Breuer
German Aerospace Center, Institute of Planetary Research, Germany

Introduction

The early Moon was covered by a global lunar magma ocean (LMO) whose solidification set the initial stage for the subsequent thermochemical evolution. Equilibrium solidification leads to a homogeneous initial mantle composition, while fractional solidification leads to a layered heterogeneous mantle composition. This difference is crucial for the subsequent thermochemical evolution of the lunar mantle and the amount of secondary crust produced. Estimates of the thickness of the secondary crust, which consists of Mg-suite rocks and basaltic lava flows, and the composition of these rocks from surface measurements and Apollo samples can be combined with models of the interior dynamics to gain insight into the evolution of the lunar mantle.

In our study we model the solid state convection in the lunar mantle and focus on the mixing and partial melt production during convection. We consider both a homogeneous initial mantle composition, as it was used in previous studies (e.g., Ziethe et al., 2009), and a heterogeneous mantle composition that formed by fractional crystallization of the LMO.

We compute the amount of partial melt and compare our results to estimates of the Moon's secondary crust. This allows us to constrain parameters such as the initial temperature for the homogeneous case and the temperature dependence of the viscosity for the heterogeneous case. Our models can provide critical information about the location and timing of partial melt, and for the more realistic heterogeneous case, also about the components that undergo melting.

Petrological modeling

For the initial mantle composition in the homogeneous lunar mantle case we chose KLB-1 peridotite (Zhang and Herzberg, 1994). The solidus, liquidus and density change due to mantle depletion were calculated with alphaMELTS. The initial temperature profiles vary from a cold to an intermediate temperature following Laneuville et al. (2013) (Figure 1b).

For the heterogeneous lunar mantle case we follow the approach described by Schwinger and Breuer (2021) to compute the fractional solidification of the LMO using the bulk lunar mantle composition of O'Neil (1991). The resulting compositional structure of the mantle consists of 5 layers, for which the predominant minerals are shown in Figure 1c. For each of these layers we calculate an average density, solidus and liquidus profiles, and their changes due to mantle depletion. The initial temperature profile follows the crystallization temperatures of the cumulates (Figure 1d).

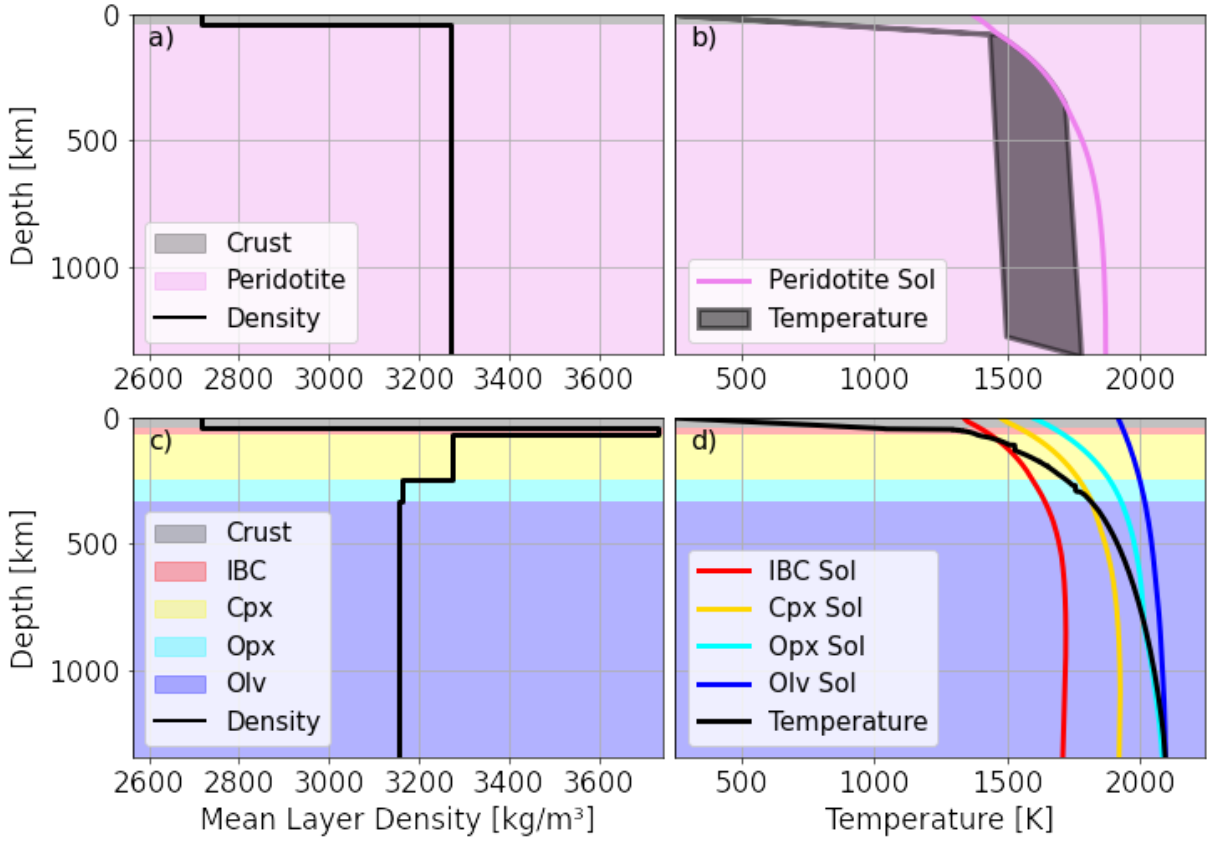

Figure 1: The initial input for the homogeneous case is shown in the upper part of the figure (panels a and b) and for the heterogeneous case in the lower part (panels c and d). The left side (panels a and c) shows the compositional layers and the density profile of the respective cases, while the right side (panels b and d) shows the solidi and the initial temperatures for the respective cases. For the homogeneous case we tested a range of initial temperatures. For the heterogeneous case the compositional mantle structure consists of 5 layers, where the predominant minerals (from core to surface) are olivine (Olv), orthopyroxene (Opx), clinopyroxene (Cpx), clinopyroxene and ilmenite (ilmenite bearing cumulates = IBC) and plagioclase (crust), respectively. The abbreviation Sol denotes the solidus.

Geodynamical modeling

We use the mantle convection code GAIA (Hüttig et al., 2013) to model the thermochemical evolution of the lunar mantle for both the homogeneous and heterogeneous case. We solve the conservation equations of mass, linear momentum, thermal energy, and composition using the extended Boussinesq Approximation in a 2D quarter cylinder geometry. The temperature- and depth-dependent viscosity follows an Arrhenius law, and we track material properties (e.g., melting temperature, density, degree of depletion, amount of heat producing elements) employing a particle-in-cell method (Plesa et al., 2013).

All simulations consider core cooling and radioactive decay. Additionally, we account for latent heat consumption during mantle melting and the increase of solidus and density changes due to mantle depletion (Breuer et al., 2018). Our models track the timing and depth of the melting events and the components that melt.

Produced melt forms the secondary crust and successful models must fit the secondary crust thickness with values between 2 to 10 km. This range accounts for basaltic lava flows that comprise less than 1% of today's crust (Head, 1976) and the Mg-suite rocks that may comprise 6% to 30% (Tompkins and Pieters, 1998, Wieczorek and Zuber, 2001). Though, recent findings show that at

least some rocks of the Mg-suite are impact melts (White et al., 2020).

Results

For the homogeneous case, our models show that a relatively cold initial potential mantle temperature of 1501 - 1547 K is required to match the secondary crust estimates of 2 to 10 km. The cold temperatures correspond to abnormally small initial magma ocean depths of only 106 - 145 km and are not able to produce early mantle melting as required to explain the oldest ages of basalts (Figure 2a).

For the heterogeneous case the initial temperature profile is determined by the crystallization temperatures and is thus a fixed parameter. In this case, the IBC cumulates with their high density and low solidus temperature can significantly affect convection and subsequent partial melting. We consider a reference viscosity of 1e21 Pa s. For models with a strong temperature-dependence of the viscosity (i.e., activation energy of 300 kJ/mol) the IBC remains trapped beneath the crust, and only 1.3 km of secondary crust are produced. In contrast, if we consider a lower temperature-dependence of the viscosity (i.e., activation energy of 83 kJ/mol), then up to 61% of IBC sinks into the mantle, producing an average secondary crust thickness of up to 2.9 km (Figure 2b).

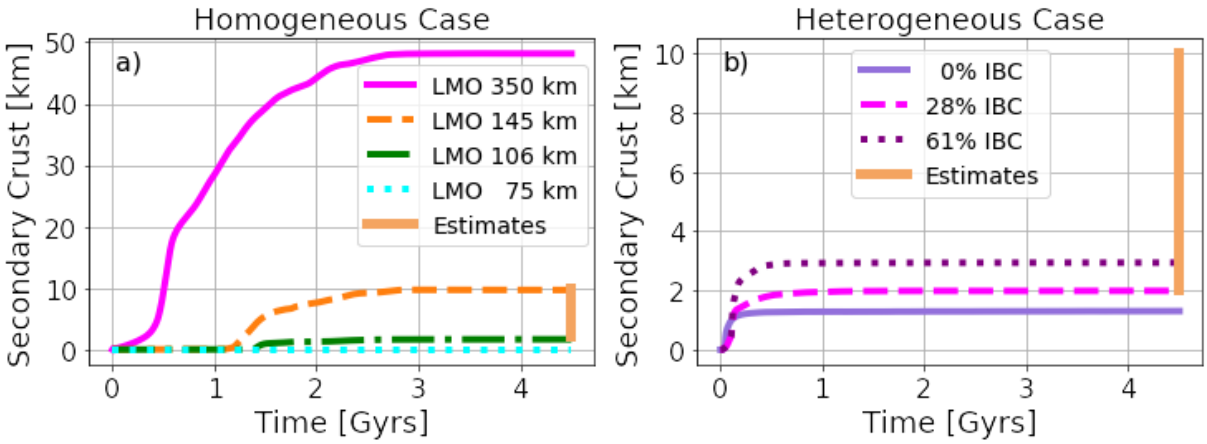

Figure 2: Constraining the homogeneous (panel a) and the heterogeneous case (panel b) with the secondary crust estimates.
For the homogeneous case, we show 4 models: the pink line with an initial LMO depth of 350 km corresponds to an intermediate potential mantle temperature of 1696 K, the orange model (LMO depth 145km) to 1547 K, the green model (LMO depth 106 km) to a potential temperature of 1501 K and the cyan line (LMO depth 75 km) to 1429 K.
For the heterogeneous case, 3 models are shown with different amounts of the IBC layer sinking into the mantle. The later is controlled by the temperature dependence of the viscosity, which is given by the activation energy. 0% IBC corresponds to an activation energy of 300 kJ/mol, 28% IBC corresponds to 100 kJ/mol, and 61% IBC to 83 kJ/mol.

Conclusion and Outlook

Our coupled petrological-geodynamical models indicate that a heterogeneous mantle composition yields more comparable results to estimates of the secondary crustal thickness than a homogeneous mantle. In the heterogeneous case, at least part of the IBC layer needs to be recycled into the mantle to match the estimates, indicating a low activation energy e of the viscosity, a low reference viscosity or additional mechanisms to destabilize the IBC layer. In the homogeneous case, our models show that only cold initial temperatures can produce a secondary crust thickness comparable to the estimates - but these are not consistent with the timing of secondary crust formation.

In future work, we will investigate the composition of the partial melt over time using the thermodynamic software Perple_X and compare our results to the composition of mare basalts. In

addition, we plan to test the consequences of a heterogeneous shallow magma ocean on the thermochemical evolution and mantle melt production.

Future missions that could return additional information about the thickness and composition of the secondary crust would greatly help to improve our numerical models and constrain the thermochemical history of the Moon.

Acknowledgements

I.B. and S.S. were supported by DFG SFB-TRR170, (subprojects C4 and A5).